Radiography of a K_α X-ray source generated through ultrahigh picosecond laser–nanostructure target interaction

Jian Wang (王 剑)[1,2], Zongqing Zhao (赵宗清)[2,*], Weihua He (何卫华)[2], Bin Zhu (朱 斌)[2], Kegong Dong (董克攻)[2], Yuchi Wu (吴玉迟)[2], Tiankui Zhang (张天奎)[2], Gao Niu (高 牛)[2], Kainan Zhou (周凯南)[2], Na Xie (谢 娜)[2], Weimin Zhou (周维民)[2], and Yuqiu Gu (谷渝秋)[2]

[1]*Department of Physics, Fudan University, Shanghai 210433, China*

[2]*Research Center of Laser Fusion, China Academy of Engineering Physics, Mianyang 621900, China*

**Corresponding author: 498427431@qq.com*

Received October 8, 2014; accepted December 22, 2014; posted online February 24, 2015

Laser-driven ultrafast X-ray sources are widely used for diagnostic radiography. However, there is a large divergence of fast electrons when they are generated by an intense short-pulse laser interacting with a foil target. We design a nanowire array target to achieve a more compact point X-ray source. Fast electrons are confined and guided by the nanowire array structure in order to generate a K_α source with a small spot size. In our work, the smallest measured source size is comparable to the laser spot size, while the conversion efficiency can reach 2.4×10^{-4}.

OCIS codes: 100.0100, 340.0340.

doi: 10.3788/COL201513.031001.

Laser-driven ultrafast X-ray sources are widely used for diagnostic radiography in high-energy density physics, X-ray scattering, inner shell photoionization[1,2], ultrafast biomedical imaging[3,4], the probing of lattice dynamics[5], and basic research in radiation biology[6]. Developing a bright laser-driven X-ray source with high resolution is necessary for the previously mentioned applications. The K_α emission mechanism using a high-intensity laser is a promising way of creating several tens of kiloelectron volts (keV), bright, laser-driven X-ray sources. When fast electrons that are generated by an intense laser impinge on a dense target material, K_α or K_β emission is generated for electrons with energies exceeding the K-shell binding energy[7]. However, such electrons are prone to spread outside of the region under direct laser illumination. Thus, the K_α source is usually 5–10 times larger than the laser focus spot size[8].

Many special targets are proposed to control the spot size of the photons K_α or K_β emission by different groups over the world, such as a wire-like target or thin target viewed edge-on[8–10]. However, the laser–photon conversion efficiencies (CEs) of these sources are limited to 10^{-5}. Recently, it was found that the microstructure on the target surface can enhance the yield of the X-ray photons greatly under low laser intensity[11,12].

In this Letter, we report a metal nanowire array which is attached to a substrate to control the K_α source size under ultrarelativistic laser irradiation. This geometry possesses good collimation and guiding effects on the generated fast electrons. The typical CE of the K_α source made in this way can reach as high as 2.4×10^{-4} and the spot size can be reduced to the value that is comparable to the laser spot. Using this method, it should be possible to produce a highly efficient K_α source based on a desktop laser.

The experiments were conducted in the Xingguang-III laser facility in the Laser Fusion Center in Mianyang, China. Xingguang-III is a Nd:glass laser system delivering 3–10 ps laser pulses at 1053 nm with energies up to 500 J. The measured intensity contrast ratio by a photodiode between the main pulse and nanosecond-level prepulse is 10^4–10^6 in our work. The *s*-polarized main laser pulses were focused on a copper target with an f/3 fixed aperture of the parabolic mirror 3. The obliquely incident laser was incident on a target at 10° from the target normal. About 30% of the energy was contained in an elliptic spot of size 20 μm × 12 μm [Fig. 1(a), inset]. The copper nanowire array targets were fabricated by an electrophoretic deposition technique on a copper substrate. When the targets are prepared, porous anodic aluminum oxide templates were used. According to the simulations results in Ref. [13], we adopted the length of the nanowire as 10–20 μm and the diameter of the nanowire as 200 nm, respectively. The space between the nanowires is also 200 nm.

In our work, the absolute source production was measured by a separated calibrated single-counting X-ray CCD which was placed in the rear of the target. The single-counting means the photon is captured in a single pixel or a few adjacent pixels and the total deposited intensity is proportional to the incoming X-ray photon energy. Thus, we can acquire the total photon number incident on the CCD from a histogram of the pixels at the same intensity level. Assuming isotropic emission in space, the CE of the source can be expressed by

$$\eta = E_K/E_L = 4\pi N \varepsilon_k / E_L \varepsilon_1(v)\varepsilon_2(v)\Omega, \tag{1}$$

where N is the photon number, E_L is the laser energy, ε_k is the energy of a single copper K_α photon, $\varepsilon_1(v)$ is the

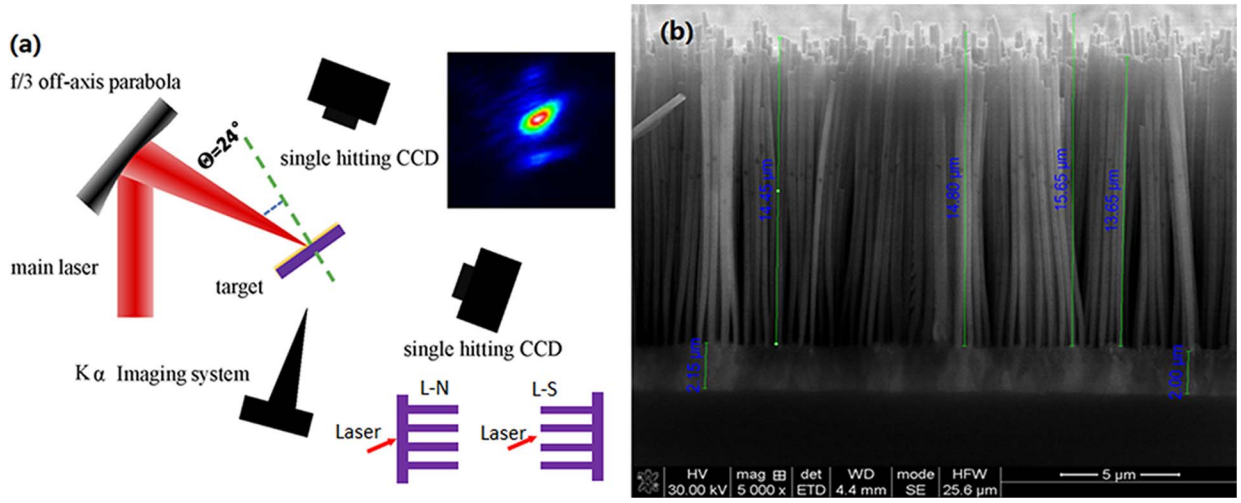

Fig. 1. (a) Schematic overview of the experiment setup. L–N means the laser is interacting with the nanowire structure directly. L–S means the laser is interacting with the substrate; (b) scanning electron microscopy image of the nanowire array target.

quantum efficiency of the CCD, $\varepsilon_2(v)$ is the transmission for the filters (including a 100 μm thick copper filter), and Ω is the solid angle of the selected area on the CCD.

Figure 2(a)shows a typical K-shell line spectrum obtained by a single-photon counting CCD in the rear side of the target. Both the Cu K_α and K_β lines are clearly distinguished. According to Eq. (1), we can calculate the CE from the K_α yields in Fig. 2(b). For the case of 94.8 J, the yield is about 1.0×10^{10}/shot/J/sr. Thus, the calculated CE is 1.5×10^{-4}. This value is consistent with many previously published data. That is, the introduction of the nanowire structure indeed does not affect the CE of the source. Furthermore, it seems that the CE is not obviously dependent on the laser energy, which means that we can always achieve a source with high CE for a laser intensity of 10^{18}–10^{19} W/cm^2. As stated previously, in our work, there exist relatively strong prepulses. Thus, the large-scale preplasmas formed in front of the target may reduce the signals, especially at an energy that is larger than 150 J, as Fig. 2(b) shows. It should be noted that if we let the laser interact with the nanowire array directly at 20 J, the CE can even be enhanced to 2.4×10^{-4}, 2–3 times larger than the value at the same laser energy, as we expect. Furthermore, the CE is higher than the highest CE at 94.8 for the Laser–Substrate (L–S) case. According to Ref. [10], the enhanced local electric fields in the surface may account for the enhancement in this case. Therefore, it is suggested that the Laser–Nanowire (L–N) interaction is more beneficial for the projected radiography.

To measure the spot size of the K_α source, we use coded imaging technology[14]. A single-photon counting X-ray CCD camera with 1340 pixels × 1300 pixels and a 50 μm thick tantalum code plate were contained in the imaging system. The system magnification was 5.8×. The camera view was 22° off the target normal. The resolution of the coded imaging system was 2 μm. A group of copper filters was placed in front of the CCD camera to ensure the detection of K_α emission. The CCD was not operated under the single-photon counting mode in the imaging process.

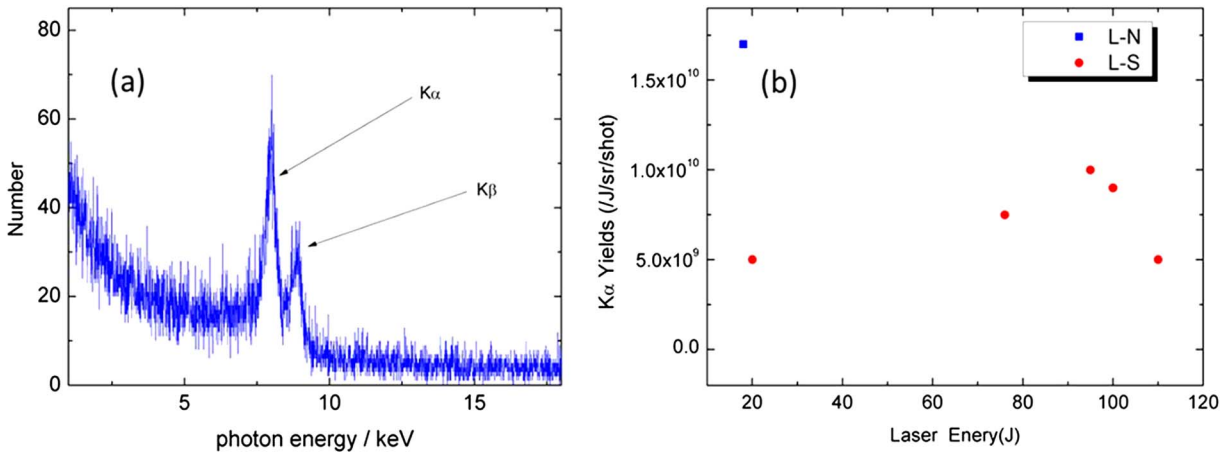

Fig. 2. (a) Spectrum of K-shell lines obtained for 94.8 J laser incidence on the target with 20 μm nanowires; (b) dependence of the total count of Kα on the laser energy for the target with 20 μm nanowires.

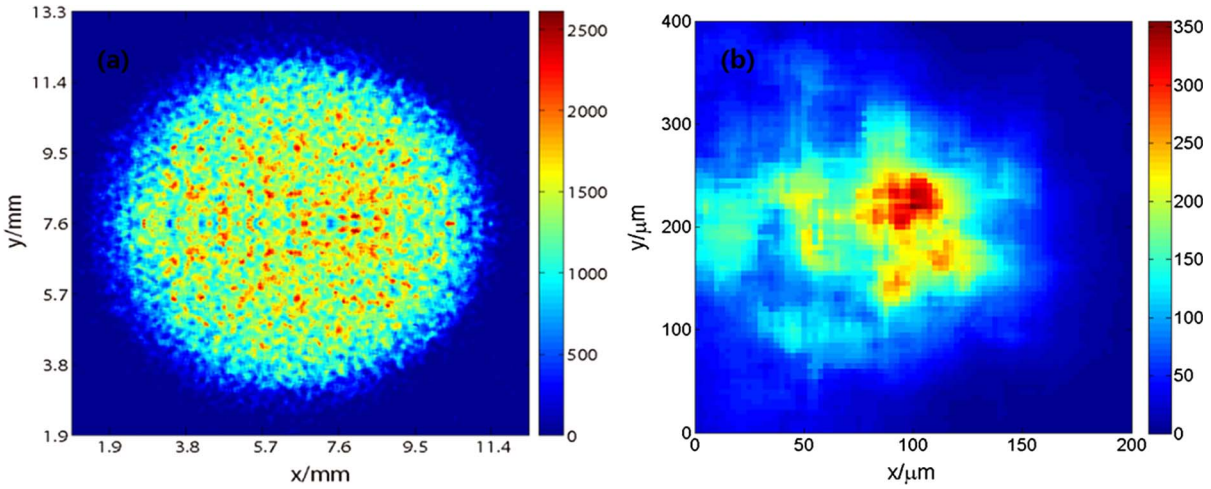

Fig. 3. (a) Original K_α image for a nanowire array target with 10 μm long nanowires and a 5 μm thick substrate. Corresponding laser peak intensity is 1×10^{19} W/cm^2; (b) restored image from (a).

Figure 3(a) shows a typical coded K_α image from the target with 20 μm long nanowires at the rear side. The corresponding peak intensity of the laser is about 1×10^{19} W/cm^2. For deconvoluting original data, we develop a blind restoration algorithm[14]. Figure 3(b) is the deconvoluted result from Fig. 3(a). As shown in Fig. 3(b), the Gaussian fitted spot size of the K_α source is about 32 μm (FWHM), which is just comparable to the laser spot size. In fact, there exists a quasi-static electromagnetic field array in the nanowire array, which is attached to the rear side of the substrate. Therefore, most of the fast electrons are confined at the nanowire surfaces and transport forward. More importantly, due to the divergent property of the beams, the magnitudes of the generated fields decrease with the target depth. The lateral momenta of the electrons convert into the forward momenta through the Lorenz force and they cannot recover their initial values[13]. Therefore, the fast electrons can be guided and collimated efficiently in the gaps between the nanowires and the spot sizes of the K_α source are reduced. A similar guiding and collimating mechanism is also reported in Ref. [14]. In contrast, for the planar target, some previous published data under similar experimental conditions shows that the spot size of the K_α source is about 5–10 times larger than the laser spot size[8].

Figure 4 is the proof-of-principle radiography result by using the K_α source in Fig. 3(b). In order to demonstrate radiography, we fabricated a test pattern consisting of a stack of 1D slits (50, 100, 200, and 300 μm) on a 50 μm thick Ta substrate in Fig. 4(a). The edges of the grids served as knife-edge targets for testing the resolution. Figure 4(b) illustrates the horizontal line-outs for the point projection radiography. The Femi fitting result of the peak indicated by the red arrow shows the FWHM of the point spread function (PSF) to be 48.9 μm. It means that the minimum of the spatial resolution reaches at least 50 μm for the point projection radiography. It should be noted that the sizes of the PSFs are larger than the observed spot size and independent of the laser energy, as Table 1 shows. For the bremsstrahlung (i.e., "deceleration

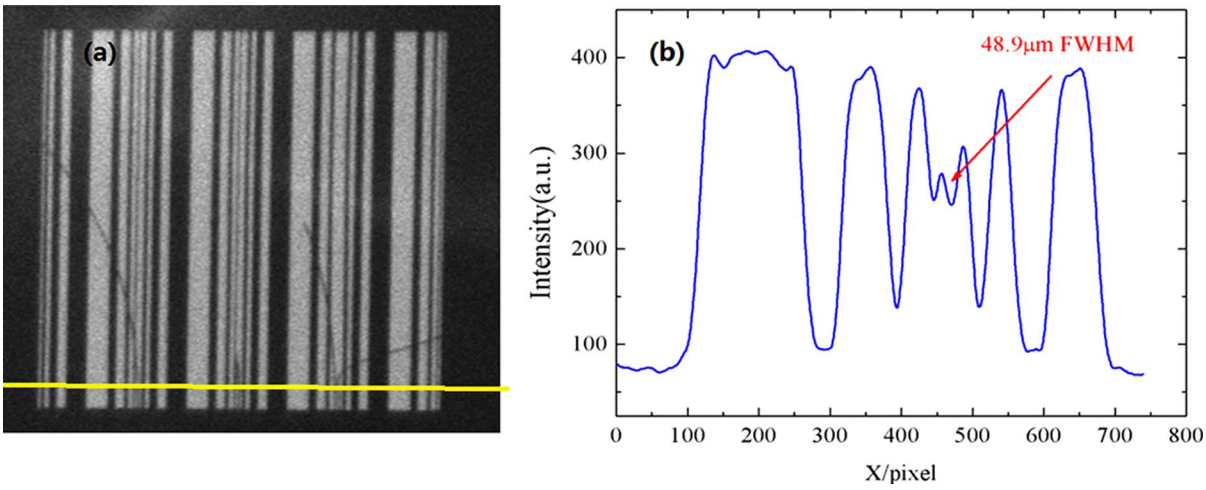

Fig. 4. (a) Stack of 1D slits (50, 100, 200, and 300 μm) on a 50 μm thick Ta substrate; (b) horizontal line-outs for the point projection radiography.

Table 1. Laser Energy versus FWHM of the PSF and CE

Laser Energy (J)	FWHM of the Point Spread Function (μm)	CE
19	43.8	2.4×10^{-4}
75	48.9	1.2×10^{-4}
94	46.4	1.6×10^{-4}

radiation") background produced in the work, the 50 μm thick Ta substrate is too thin to hinder the high-energy photons. Therefore, blur of the knife edge may occur and the deduced PSFs are larger than the spot size of the source. Additionally, the imperfection of the knife edge also accounts for the discrepancy between the PSFs and the source size. According to the simulation results in Ref. [12], most of the fast electrons can be guided and collimated for laser intensity from 1×10^{18} to 1×10^{20} W/cm^2, thus the deduced PSFs seem to be independent of the laser intensity, in contrast to the results in Ref. [15].

In conclusion, we demonstrate a reduction in the K_α X-ray source size with good CE. The quasi-static electromagnetic fields at the surface of the nanowires confines and guides relativistic electrons, greatly reducing the divergence. The multiwire structure can maintain the source CE at the same level as that of a thin foil target. Therefore, the smallest source size achieved is about 30 μm with a source CE of 2.4×10^{-4}. This efficiency is comparable to that obtained in previous work. Besides X-ray radiography applications, the nanowire target can be used in wakefield injection[16] and terahertz radiation generation[17].

We would like to thank the staff of the Xingguang-III Group for their support in laser system operation. We also thank G. Niu for target fabrication. This work was supported by the National Science Foundation of China (Grant Nos. 1174259, 11175030, 11475030, and 10905051), the Science and Technology on Plasma Physics Laboratory (Grant No. 9140c680306120c68253), and the China Academy of Engineering Physics Foundation (Grant No. 2011B0102021).

References

1. S. Moon and D. Eder, Phys. Rev. A **57**, 1391 (1998).
2. S. Fujioka, H. Takabe, N. Yamamoto, D. Salzmann, F. Wang, H. Nishimura, Y. Li, Q. Dong, S. Wang, Y. Zhang, Y.-J. Rhee, Y.-W. Lee, J.-M. Han, M. Tanabe, T. Fujiwara, Y. Nakabayashi, G. Zhao, J. Zhang, and K. Mima, Nat. Phys. **5**, 821 (2009).
3. J. Kieffer, A. Krol, Z. Jiang, C. Chamberlain, E. Scalzetti, and Z. Ichalalene, Appl. Phys. B **74**, S75 (2002).
4. T. Pikuz, A. Faenov, S. Magnitskiy, N. Nagorskiy, M. Tanaka, M. Ishino, M. Nishikino, Y. Fukuda, M. Kando, Y. Kato, and T. Kawachi, High Power Laser Sci. Eng. **2**, e12 (2014).
5. K. Sokolowski-Tinten, C. Blome, J. Blums, A. Cavalleri, C. Dietrich, A. Tarasevitch, I. Uschmann, E. Förster, M. Kammler, M. Horn-von-Hoegen, and D. von der Linde, Nature **422**, 287 (2003).
6. M. Nishikino, K. Sato, N. Hasegawa, M. Ishino, S. Ohshima, Y. Okano, T. Kawachi, H. Numasaki, T. Teshima, and H. Nishimura, Rev. Sci. Instrum. **81**, 026107 (2010).
7. N. L. Kugland, C. G. Constantin, P. Neumayer, H.-K. Chung, A. Collette, E. L. Dewald, D. H. Froula, S. H. Glenzer, A. Kemp, A. L. Kritcher, J. S. Ross, and C. Niemann, Appl. Phys. Lett. **92**, 241504 (2008).
8. H. S. Park, D. M. Chambers, H.-K. Chung, R. J. Clarke, R. Eagleton, E. Giraldez, T. Goldsack, R. Heathcote, N. Izumi, M. H. Key, J. A. King, J. A. Koch, O. L. Landen, A. Nikroo, P. K. Patel, D. F. Price, B. A. Remington, H. F. Robey, R. A. Snavely, D. A. Steinman, R. B. Stephens, C. Stoeckl, M. Storm, M. Tabak, W. Theobald, R. P. J. Town, J. E. Wickersham, and B. B. Zhang, Phys. Plasmas **13**, 056309 (2006).
9. H. S. Park, B. R. Maddox, E. Giraldez, S. P. Hatchett, L. T. Hudson, N. Izumi, M. H. Key, S. Le Pape, A. J. MacKinnon, A. G. MacPhee, P. K. Patel, T. W. Phillips, B. A. Remington, J. F. Seely, R. Tommasini, R. Town, J. Workman, and E. Brambrink, Phys. Plasmas **15**, 072705 (2008).
10. K. Vaughan, A. S. Moore, V. Smalyuk, K. Wallace, D. Gate, S. G. Glendinning, S. McAlpin, H. S. Park, C. Sorce, and R. M. Stevenson, High Energy Density Phys. **9**, 635 (2013).
11. S. Mondal, I. Chakraborty, S. Ahmad, D. Carvalho, P. Singh, A. Lad, V. Narayanan, P. Ayyub, and G. R. Kumar, Phys. Rev. B **83**, 035408 (2011).
12. G. Kulcsár, D. AlMawlawi, F. W. Budnik, P. R. Herman, M. Moskovits, L. Zhao, and R. S. Marjoribank, Phys. Rev. Lett. **84**, 5149 (2000).
13. J. Wang, Z. Q. Zhao, B. Zhu, B. Zhang, Z. M. Zhang, W. M. Zhou, and Y. Q. Gu, Phys. Plasma **21**, 103111 (2014).
14. W. H. He, Z. Q. Zhao, J. Wang, B. Zhang, F. Qian, M. Shui, F. Lu, J. Teng, L. F. Cao, and Y. Q. Yu, Opt. Express **22**, 5875 (2014).
15. J. S. Green, V. M. Ovchinnikov, R. G. Evans, K. U. Akli, H. Azechi, F. N. Beg, C. Bellei, R. R. Freeman, H. Habara, R. Heathcote, M. H. Key, J. A. King, K. L. Lancaster, N. C. Lopes, T. Ma, A. J. MacKinnon, K. Markey, A. McPhee, Z. Najmudin, P. Nilson, R. Onofrei, R. Stephens, K. Takeda, K. A. Tanaka, W. Theobald, T. Tanimoto, J. Waugh, L. Van Woerkom, N. C. Woolsey, M. Zepf, J. R. Davies, and P. A. Norreys, Phys. Rev. Lett. **100**, 015003 (2008).
16. W. Wang, Z. Sheng, Y. Li, Q. Dong, X. Lu, J. Ma, and J. Zhang, Chin. Opt. Lett. **9**, 110002 (2011).
17. K. Nakajima, H. Lu, X. Zhao, B. Shen, R. Li, and Z. Xu, Chin. Opt. Lett. **11**, 013501 (2013).